*Mechatronic Systems and Control, Vol. 52, No. 10, 2024*
*An Open Access Paper*

# RESEARCH ON 6-DOF MOTION SYSTEM OF UNMANNED HELICOPTER

Hongcheng Zhou*

## Abstract

The flight dynamics of unmanned helicopters are the core of their dynamic simulation system. In response to the linearised equation of the unmanned helicopter given, a closed-loop control law for the attitude control loop and speed control loop was designed by introducing state feedback, while satisfying the controllability and observability of the system. The helicopter was transformed from a static unstable object to a stable and controllable object. A 6-DOF motion simulation strategy for the unmanned helicopter circuit and autopilot circuit was proposed, and the unmanned helicopter control system was combined with a 6-DOF motion simulation platform to construct a 6-DOF motion simulation system for unmanned helicopters. Simulation experiments were conducted on typical flight modes of unmanned helicopters, and the simulation results showed that the robustness of the system was greatly improved.

## Key Words

Unmanned helicopter, attitude control loop, speed control loop, state feedback

## 1. Introduction

Unmanned helicopters are an important member of the drone family, possessing the common advantages of both drones and helicopters, and have incomparable advantages compared to conventional layout drones. Unmanned helicopters have low requirements for the area and quality of the site during take-off and landing and can achieve forward and backward flight, left and right flight, and hover flight at fixed points within the flight mission profile, as well as achieve *in situ* turning of the hovering point. The above advantages of unmanned helicopters make them more versatile compared to fixed wing drones. In military applications, unmanned helicopters can be used in fields, such as battlefield reconnaissance, communication relay, missile guidance, and firepower attacks. In terms of civilian use, unmanned helicopters can be used for resource detection, meteorological monitoring, power rescue, aerial photography, medical aid, and other fields [1].

The flight control system and sensor devices are the core parts of the entire unmanned helicopter system. The control performance, stability, reliability, and sensor accuracy of the flight control system are important guarantees for the flight quality of the unmanned helicopter, and also the key to determining the smooth completion of the entire flight mission. Scholars have conducted research on these aspects [2]. Hasan *et al.* [3] addressed the design of ADRC for UAV based on three types of extended state observers. Zheng [4] has suggested that combines traditional PID control with genetic algorithms, which can improve the traditional PID control. Gupta and Dewan [5] have eliminated the chattering, control discontinuity is smoothened in a boundary layer by the proposed sigmoid-based quasi-sliding mode method. Although the PID control algorithm has a simple structure and a wide range of applications. However, for unmanned helicopters, which are prone to changes in their own parameters (such as mass and inertia coefficient) and are susceptible to external environmental disturbances that alter the dynamic model, PID cannot adapt due to its fixed and unchanged gain coefficient, making it difficult to maintain good stability of the control system. Many control algorithms with superior control performance, including a series of nonlinear control methods, such as backstepping, sliding mode control, and adaptive control, are applied in helicopter research. However, the engineering practicality of the above flight control algorithms still needs to be further improved and enhanced [6]. It is an important experimental equipment for the development of unmanned helicopter flight control systems and semi physical simulation experiments.

The contribution of this article is reflected here. This article investigates the attitude and altitude tracking control problem of unmanned helicopter systems with disturbances, achieving asymptotic tracking of attitude and altitude. Design an interference observer to estimate the unknown interference that affects each channel. Then, by incorporating backstepping control technology, a controller is proposed to achieve attitude and altitude anti-interference tracking of targets. Finally, the effectiveness

* School of Electronic and Information Engineering, Jinling Institute of Technology, Nanjing 211169, China; e-mail: zhouhcnj@163.com
Corresponding author: Hongcheng Zhou

*(DOI: 10.2316/J.2024.201-0442)*

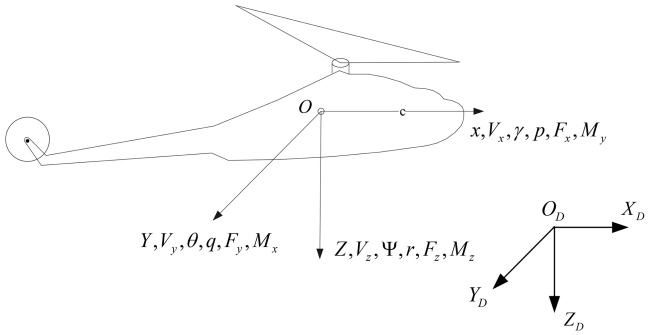


Figure 1. Helicopter ground axis and airframe coordinate system.

of the proposed control scheme and its superiority over conventional feedback control techniques were verified through MATLAB simulation.

## 2. The Kinetic Equation of Unmanned Helicopter

### 2.1 Full Motion Equation of Unmanned Helicopter

The helicopter flight dynamics regards the helicopter as an ideal rigid body. So the helicopter in the air movement has 6-DOF, namely, the helicopter centre of the three moving DOF and the helicopter around the mass centre of the three rotational DOF [7]. Accordingly, the dynamic equation of the helicopter is composed of the movement dynamic equation of the mass centre and the dynamic equation of the helicopter rotating around the mass centre.

Helicopters have many moving parts, such as rotors, tail rotor, and so on. The forces exerted by a helicopter in flight include aerodynamic force, inertial force, and gravity force. Gravity is a steady-state force, and aerodynamic and inertial forces are generated by the interaction of rotor, tail rotor, fuselage, and other components with air during helicopter flight. To study the dynamic characteristics of the helicopter, the axis coordinate system and the ground axis coordinate system are established. The coordinate system of the unmanned helicopter is shown in the Fig. 1 [8].

Let the helicopter mass $m$, the helicopter speed $V$, the total force $F$ acting on the particle. This is derived from Newton's second law [9].

The external force $F$ is composed of the aerodynamic force and gravity of the helicopter each component. The dynamic equation of the mass centre movement are obtained by decomposing the $F$ components and expressing them by $F_x$, $F_y$, $F_z$ in (1), respectively, [10].

$$\begin{cases} m(\frac{dV_x}{\mathrm{dt}} + V_z q - V_y r) + mg\sin\theta = F_x \\ m(\frac{dV_y}{\mathrm{dt}} + V_x r - V_z p) + mg\cos\theta\cos\gamma = F_y \\ m(\frac{dV_z}{\mathrm{dt}} + V_y p - V_x q) - mg\cos\theta\sin\gamma = F_z \end{cases} \tag{1}$$

To study the rotation of a helicopter around the mass centre, the momentum of the helicopter to the origin is $H$, and the moment sum of the force acting on the helicopter to the origin is $M$ (2). It is derived from the momentum theorem.

$$m\frac{\mathrm{dH}}{\mathrm{dt}} = M \tag{2}$$

By decomposing the torque along the body coordinate axis, the dynamic (3) of the helicopter rotating around the mass centre are obtained.

$$\begin{cases} I_x\dot{p} + \mathrm{qr}(I_z - I_y) - I_{\mathrm{xz}}(\dot{r} + pq) = M_x \\ I_y\dot{q} + \mathrm{pr}(I_x - I_z) + I_{\mathrm{xz}}(p^2 - r^2) = M_y \\ I_z\dot{r} + \mathrm{pq}(I_y - I_x) - I_{\mathrm{xz}}(\dot{p} - qr) = M_z \end{cases} \tag{3}$$

Equations (2) and (4) in differential equation form (4):

$$\begin{cases} \dot{V}_x = V_y r - V_z q - g\sin\theta + F_x/m \\ \dot{V}_y = V_z p - V_x r - g\cos\theta\cos\gamma + F_y/m \\ \dot{V}_z = V_x q - V_y p + g\cos\theta\sin\gamma + F_z/m \\ \dot{p} = -(\mathrm{qr}(I_z - I_y) - I_{\mathrm{xz}}(\dot{r} + pq))/I_x + M_x/I_x \\ \dot{q} = -(\mathrm{pr}(I_x - I_z) + I_{\mathrm{xz}}(p^2 - r^2))/I_y + M_y/I_y \\ \dot{r} = -(\mathrm{pq}(I_y - I_x) - I_{\mathrm{xz}}(\dot{p} - qr))/I_z + M_z/I_z \end{cases} \tag{4}$$

The kinematic relationship between the attitude angle and the angular velocity of a helicopter can be described by the following (5).

$$\begin{cases} \dot{\theta} = q\cos\gamma - r\sin\gamma \\ \dot{\gamma} = p + \tan\theta(q\sin\gamma + r\cos\gamma) \\ \dot{\psi} = (q\sin\gamma + r\cos\gamma)\mathrm{sec}\theta \end{cases} \tag{5}$$

The (4) and (5) form the 9th order nonlinear motion equation of the helicopter, where, the axis speed $V_x$, $V_y$, $V_z$ of the airframe, the pitch angle $\theta$, the roll angle $\gamma$, and the yaw angle $\psi$, the pitch angle rate $p$, the roll angle rate $q$, and the yaw angle rate $r$.

### 2.2 Linearised Small Disturbance Equation for Unmanned Helicopter

The helicopter linearised small disturbance state space (6) is shown below [11].

$$\begin{aligned} \dot{x} &= Ax + Bu \\ y &= Cx \end{aligned} \tag{6}$$

Where: the state matrix $A$, for the input matrix $B$, the output matrix $C$, the state vector $x = [V_x, V_y, V_z, p, q, r, \gamma, \theta, \psi]^T$, the control input $u = [\Delta\varphi_M, \Delta B_1, \Delta A_1, \Delta\varphi_T]^T$. This paper presents a linear small disturbance model of an unmanned helicopter in hovering flight mode. The matrix $A$ and $B$ in (7) are shown below [12].

$$A = \begin{bmatrix} 0 & 0 & 0 & 0 & 0 & 0 & 1.0000 & -0.0004 & 0.0089 \\ 0 & 0 & 0 & 0 & 0 & 0 & 0 & 0.9989 & -0.0089 \\ 0 & 0 & 0 & 0 & 0 & 0 & 0 & -0.0459 & 0.999 \\ 0 & -9.7996 & 0 & -0.0376 & 0.0012 & 0.0039 & -0.1854 & 0.1858 & 0.0002 \\ 9.7893 & 0.004 & 0 & 0.0243 & -0.0224 & -0.0035 & -0.1879 & -0.2498 & -0.5589 \\ 0.45 & -0.0873 & 0 & -0.0176 & -0.0224 & -0.4148 & -0.0049 & 0.5223 & 0 \\ 0 & 0 & 0 & -0.0042 & -0.1964 & -0.0113 & -2.0155 & -2.0534 & 0.0530 \\ 0 & 0 & 0 & 0.0420 & 0.0040 & -0.0001 & 0.4760 & -0.4598 & 0 \\ 0 & 0 & 0 & -0.2175 & -0.1334 & 0.0196 & -0.0699 & 0.3255 & 0.564 \end{bmatrix}$$

$$B = \begin{bmatrix} 0 & 0 & 0 & 0 \\ 0 & 0 & 0 & 0 \\ 0 & 0 & 0 & 0 \\ 0.9367 & 9.8644 & -0.0572 & 0 \\ -0.1419 & -0.3046 & 10.1427 & 4.1911 \\ -103.5045 & 0.3630 & 0.0049 & 0 \\ 5.3526 & 0.2991 & 108.4963 & -3.9151 \\ 0.1079 & -24.7949 & 0 & 0 \\ 51.0285 & 2.9408 & 3.6443 & -40.26 \end{bmatrix} \quad (7)$$

## 3. Flight Control Law Design for Unmanned Helicopter

The open-loop stability, controllability, and observability of an unmanned helicopter hover are analysed. The closed-loop control law of attitude control and speed control is designed by introducing state feedback, and the helicopter is transformed from static instability to stable controllable object [13].

### 3.1 Stability Analysis

Stability is an important characteristic of the system. This paper describes the convergence of the solution of the system equation under the initial condition when the system input is zero [14]. Let the hovering mode initial condition of the unmanned helicopter be $x = x(t_0)$, and the solution of the system (8) under the initial condition be:

$$x = \Phi(t - t_0)x(t_0) \quad (8)$$

Where: the system state transition matrix $\Phi(t - t_0) = e^{A(t-t_0)}$, the solution $x(t)$ of the state equation, the convergence is related to the system state matrix. When all the eigenvalues of the matrix $A$ have negative real parts, the system $x(t)$ is stable if it converges, otherwise, the $x(t)$ divergence will lead to the system instability.

As can be seen from Table 1, the hover mode state matrix $A$ has the characteristic root of the positive real part, and the system initial state is divergent. The helicopter is statically unstable, so the system needs to introduce a controller to correct it to become a stable system.

Table 1
Eigenvalue of Helicopter Hover Modal Matrix

| | Eigenvalues | | Eigenvalues | | Eigenvalues |
|---|---|---|---|---|---|
| 1 | 0 | 4 | 0.0098+0.9333i | 7 | 0.2307−0.5432i |
| 2 | −1.7973 | 5 | 0.0098−0.9333i | 8 | 0.5809 |
| 3 | −1.2359 | 6 | 0.2307+0.5432i | 9 | −0.4147 |

### 3.2 Flight Control Law Parameters Analysis for Unmanned Helicopters

The traditional PID control algorithm is still widely used because of its simplicity, reliability, obvious physical meaning, and easy realisation. When designing the control law of the unmanned helicopter flight control system, the attitude control, and speed control loop are designed according to the simulation test, and the PID control parameters are adjusted at last. It not only guarantees better dynamic quality characteristics but also gives consideration to robustness. PID parameter tuning refers to other helicopter control parameter setting, and is

continuously adjusted in the simulation test to obtain the best quality and performance.

*3.2.1 Attitude Control Loop Design*

Closed-loop attitude control has a direct impact on flight control performance. Receive the command signal from the speed loop, so that the unmanned helicopter according to the command to maintain a certain flight attitude. The pitch and roll attitude control adopts a double closed loop control loop structure, which inertial measurement unit the real-time measurement of the UAV's attitude angle and angular rate feedback signals, and the two loops, respectively, play the role of attitude control and attitude stability. In the attitude control loop, the controller sends the attitude angle control command to the unmanned helicopter through the ground control equipment.

After receiving it, the flight control computer fuses it with the attitude feedback signal, controls the angular rate increasing control loop according to certain rules, adjusts the angular velocity of the unmanned helicopter, and changes its attitude angle until the angular velocity is zero, the unmanned helicopter reached its new equilibrium position. The linear displacement output of the four rudders is converted into the corresponding variable distance, so that the rotor disk and the fan make the corresponding action, thus the attitude of the unmanned helicopter is controlled. Based on the reference materials, the closed-loop control law of pitch and roll attitude is as follows in (9) [15]:

$$\begin{cases} B_1' = \left[ \int K_{\mathrm{i}\theta} \left(\theta_g - \theta\right) \mathrm{d}t + K_\theta \left(\theta_g - \theta\right) - \omega_y \right] \times K_{\omega \mathrm{y}} \\ A_1' = \left[ \int K_{\mathrm{i}\gamma} \left(\gamma_g - \gamma\right) \mathrm{d}t + K_\gamma \left(\gamma_g - \gamma\right) - \omega_x \right] \times Kwx \end{cases} \tag{9}$$

*3.2.2 Course Control*

The course control is used to maintain or change the set course of the helicopter. When the course control works, the course feedback signal is used for the closed-loop control. To ensure the reliable operation of the heading control mode, the speed feedback control loop must be set up in the heading channel, and the damping of the heading channel must be increased to make it stable. Therefore, the heading angular rate signal is introduced into the control signal to form a heading angular rate closed loop as a heading stabilisation loop, and on this basis, a heading angular feedback loop is introduced. Based on the reference materials, it can be concluded that the control law of the course passage is shown in (10) [16].

$$\varphi_T = \left[K_\psi \left(\psi_g - \psi\right) - \omega_z\right] \times K_{\omega \mathrm{z}} + \varphi_{T0} \tag{10}$$

*3.2.3 Speed Control Loop*

For the forward speed control of a conventional helicopter, the lift and gravity generated by the rotor rotation are balanced when the helicopter is hovering in the air. In order for a helicopter to fly at a certain speed, it is necessary to change the pitch of the helicopter so that the plane of rotation of the rotor tilts forward at a certain angle, so that the lift force generated by the rotor tilts forward and the horizontal component of the lift force in the horizontal plane, the forward pull pulls the helicopter forward to accelerate. To reduce the forward speed of the helicopter so that the lift in the direction of flight component is reduced, rotor rotation plane up. Based on the reference materials, the forward speed control, and lateral speed control laws for unmanned helicopters are as follows in (11) [17]:

$$\begin{cases} \theta_g = K_{\mathrm{vx}} \left(V_{\mathrm{xg}} - V_x\right) \\ \gamma_g = K_{\mathrm{vy}} \left(V_{\mathrm{yg}} - V_y\right) \\ B_1' = K_{\omega \mathrm{y}} \left( \int K_{\mathrm{i}\theta} \left(\theta_g - \theta\right) \mathrm{d}t + K_\theta \left(\theta_g - \theta\right) - \omega_y \right) \\ A_1' = K_{\omega \mathrm{x}} \left( \int K_{\mathrm{i}\gamma} \left(\gamma_g - \gamma\right) \mathrm{d}t + K_\gamma \left(\gamma_g - \gamma\right) - \omega_x \right) \end{cases} \tag{11}$$

Where: $V_x$ and $V_y$ represent the GPS output $x$-axis and $y$-axis speed, $V_{\mathrm{xg}}$ and $V_{\mathrm{yg}}$ represent the $x$-axis and $y$-axis given command speed, respectively.

## 4. Unmanned Helicopter 6-DOF Motion Simulation

The 6-DOF motion simulation is used to reproduce the angular and linear motion of an unmanned helicopter, reveal the mathematical and physical process of helicopter flight, and realise the 6-DOF motion simulation of an unmanned helicopter. Two schemes of 6-DOF unmanned helicopter motion simulation are proposed for the mission: human-in-loop motion simulation and autopilot-in-loop motion simulation.

### 4.1 Unmanned Helicopter Flight Profiles for Motion Simulation

The unmanned helicopter can realise vertical take-off and landing, hover in the air. and fly forward and backward. It has little requirement to the airport and runway. In the military, the unmanned helicopter can perform reconnaissance and surveillance, ground attack, electronic jamming, communication relay, target location, and other tasks by carrying different mission equipment [18]. In the civil aspect, the unmanned helicopter may apply in the aviation photography, the meteorological survey, the exploration survey, the forest fire prevention and rescue, and so on. The aim of unmanned helicopter is to complete a certain flight mission, which includes several flight mode combinations of the helicopter. That includes vertical take-off, hover, maintain a certain speed or attitude before flying, hover and flight tasks, turn around, landing, and other flight modes [19]. The 6-DOF motion proposed in this paper can realise the simulation of the unmanned helicopter basic flight modes.

The 6-DOF motion simulation platform of unmanned helicopter is a system which is similar to helicopter by similarity principle in laboratory. The 6-DOF motion simulation platform designed in this paper can't completely include the simulated performance and flight envelope of the unmanned helicopter, but can realise the simulation of the key information and control characteristics of the unmanned helicopter in the ground environment.

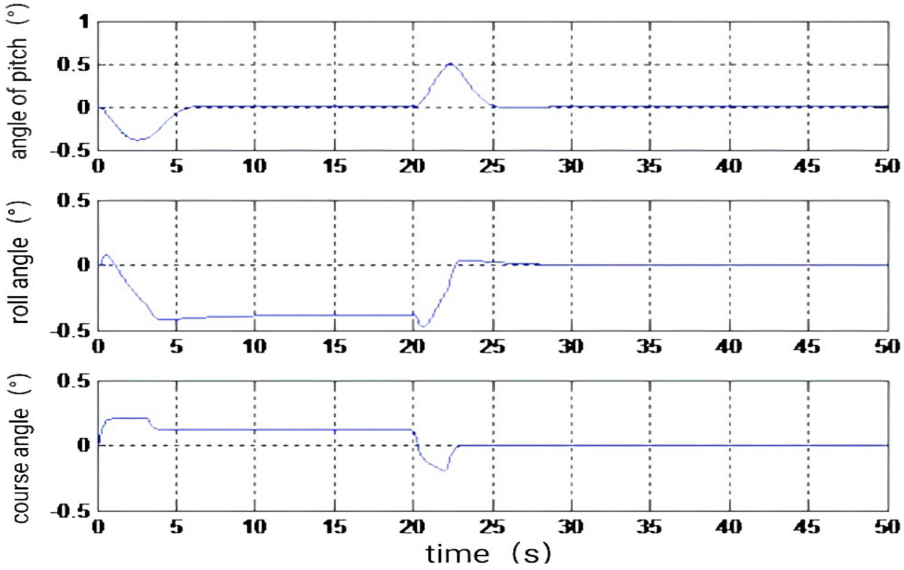


Figure 2. The angular motion response curves of helicopter take-off and hover modes.

### 4.2 The Motion Simulation of Unmanned Helicopter

The general structure and working principle of the 6-DOF motion simulation system, including the platform are deeply analysed. In this section, the platform is used for the motion simulation experiment of unmanned helicopter, two schemes for motion simulation of unmanned helicopter are proposed. The control quantity of the unmanned helicopter can be realised by the pilot through the control device or by the autopilot.

## 5. Unmanned Helicopter 6-DOF Motion Simulation

On the basis of the research on the servo control of the 6-DOF motion simulation platform and the dynamics model of the unmanned helicopter, combining the mathematical model of the unmanned helicopter with the 6-DOF motion simulation. Aiming at the 6-DOF motion simulation scheme of the unmanned helicopter, the 6-DOF motion simulation strategy is analysed, and the relevant experimental simulation data are given [20].

Based on the analysis of 6-DOF motion simulation mechanism, servo control strategy, and 6-DOF motion simulation strategy of an unmanned helicopter, for the given flight mission typical flight mode, 6-DOF motion simulation test of unmanned helicopter is carried out. The unmanned helicopter autopilot motion simulation scheme is selected to test the angular motion and line motion of platform tracking helicopter.

### 5.1 Take-off and Hover Tracking Test

Take-off mode helicopter is in speed closed-loop mode. The body $x$-axis speed is realised by pitching attitude and pitching rate, and the body $y$-axis speed is realised by rolling attitude and rolling rate. Helicopter body $x$-axis and $y$-axis speed is given in (12) [21].

$$\begin{cases} V_x = 0 \text{ m/s} \\ V_y = 0 \text{ m/s} \end{cases} \tag{12}$$

The response curves of angular motion, velocity, and displacement of the platform in hover mode after take-off are shown in Figs. 2–4, respectively.

When the given speed of the helicopter body $z$ axis changes, both the body $x$ axis and $y$ axis speed are subject to certain interference. The helicopter's northbound speed is negative and its eastbound speed is positive after being disturbed, and the expected values are all zero. The disturbance energy of the aircraft tends to zero quickly under negative pitch and roll angle corrections.

### 5.2 Direct Flight Tracking Test

After the helicopter completes the take-off process and remains in hover, the ground pilot changes the helicopter from the hover state to the direct flight state through the direct flight remote control command. The velocity of $y$-axis and $z$-axis in the direct flight is given in (13) [22].

$$\begin{cases} V_y = 0 \text{ m/s} \\ V_z = 0 \text{ m/s} \end{cases} \tag{13}$$

The helicopter flies forward steadily at a given speed, the straight flight time is set to 30 s, and the initial altitude of the straight flight mode is 100 m. The response curves of angular motion, velocity, and displacement of the modal platform are shown in Figs. 5–7, respectively.

In the process of the helicopter body $x$-axis acceleration and deceleration, the velocity of the body $y$-axis, and $z$-axis are disturbed to some extent, and the fluctuation of helicopter rise-fall velocity can reach $0.9m/s$. After the $x$ velocity stabilises, both the easterly and the up-down perturbed velocities remain stable near zero, as shown in

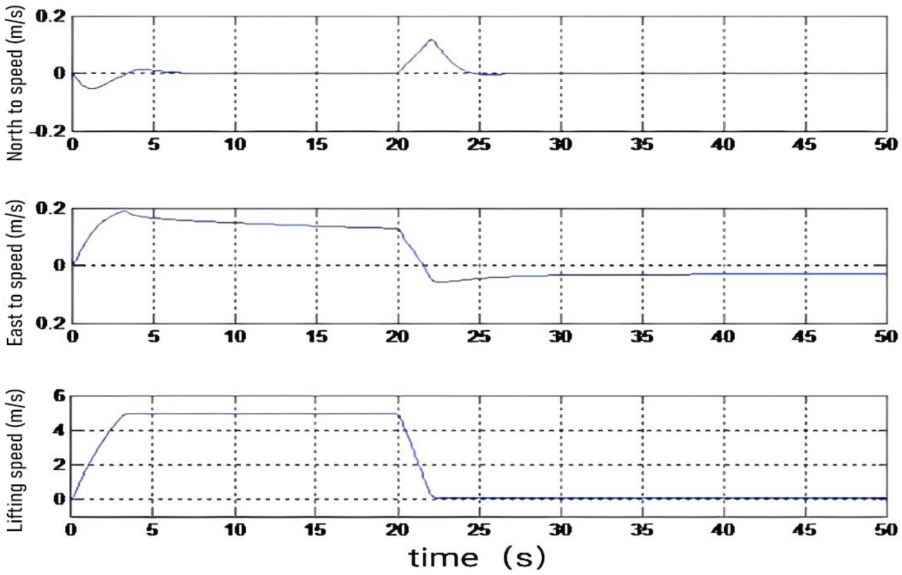


Figure 3. The velocity response curves of helicopter take-off and hover modes.

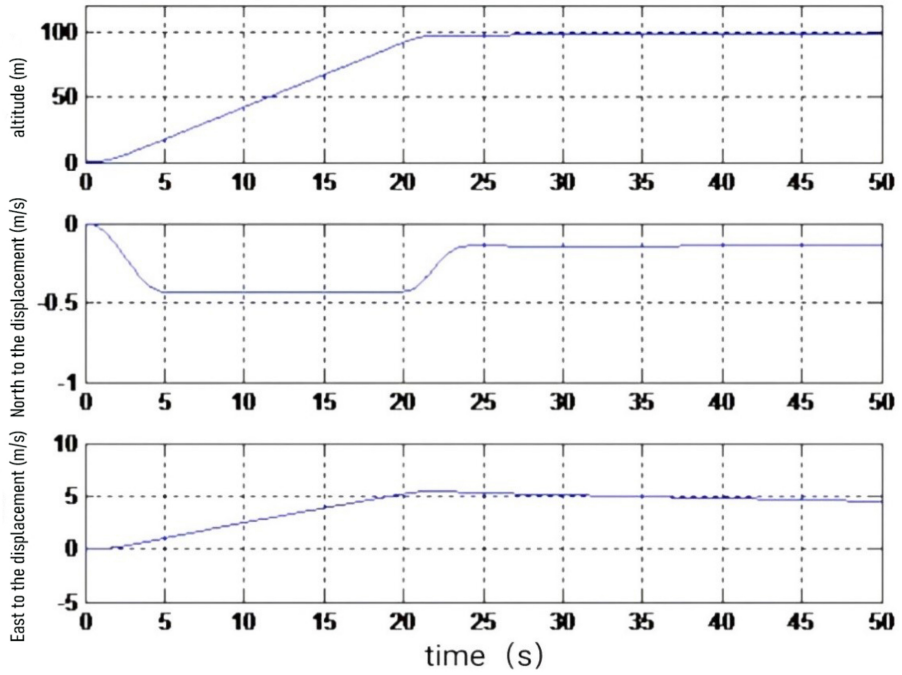


Figure 4. The displacement response curves of helicopter take-off and hover modes.

Fig. 7. The helicopter needs a negative pitch angle in the acceleration process, at which time the $z$-component of the rotor tension decreases, the helicopter occurs losing altitude phenomenon. The results are shown in Table 2.

Under the influence of nonlinear friction, the classical method is prone to low-speed crawling phenomenon in tracking low-speed signals, which reduces the platform tracking accuracy. The conventional control algorithms do not have ideal anti-interference performance for interference, and the system output cannot accurately track the expected value. The composite control design significantly improves the anti-interference dynamic characteristics of the closed-loop system, and the system output can quickly track the expected value. Compared to traditional control algorithms, composite control design improves the anti-interference dynamic characteristics and steady-state performance of closed-loop systems by more than 50%. Adjusting time, mean squared error, increase percentage of the angular motion response curves is 2.34 s, 0.0012, 63.61%, respectively. Adjusting time, mean squared error, increase percentage of the velocity response is 2.47 s, 0.0008, 71.43%, respectively. Adjusting time, mean squared error, increase percentage of the displacement response curves is 2.32 s, 0.0011, 82.62%, respectively. Other performance comparisons are shown in Table 2. We can see that the enabling precise estimation and compensation of

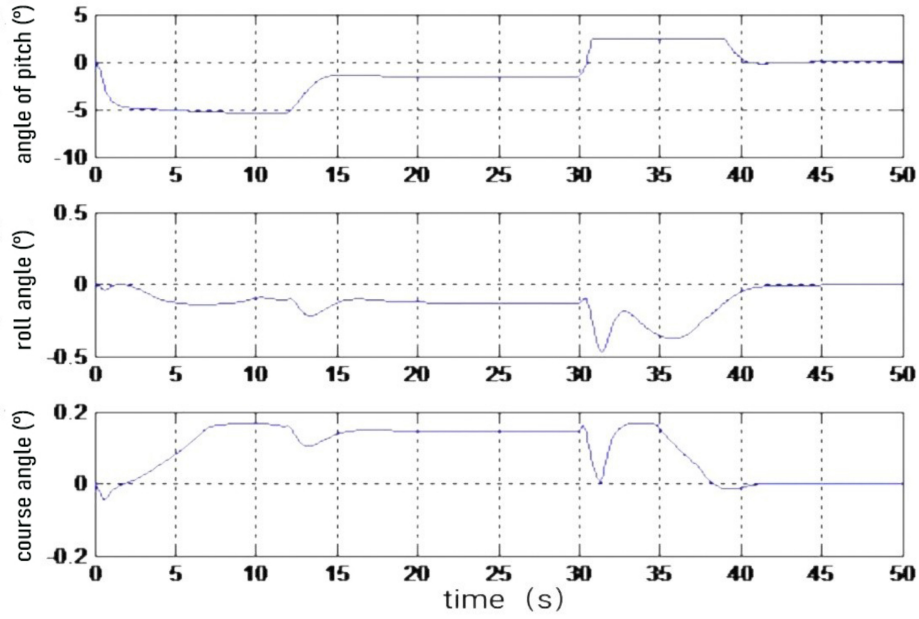


Figure 5. The angular motion response curve of the helicopter direct flight mode platform.

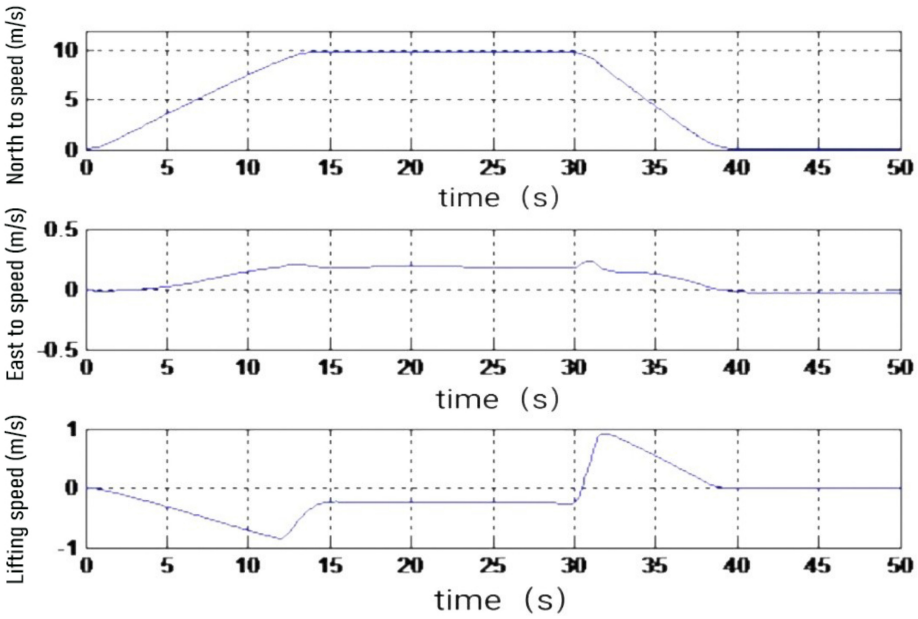


Figure 6. The velocity response curve of the helicopter direct flight mode platform.

its impact. This makes the control algorithm have better anti-interference performance, higher accuracy, and better control effect.

## 6. Conclusion

The flight control loop and control law of an unmanned helicopter are designed according to the linear small disturbance equation. The helicopter is transformed from a static unstable object to a stable controllable object. In this study, the 6-DOF motion simulation strategy for the unmanned helicopter circuit and autopilot circuit was proposed. Firstly, the open-loop stability, controllability, and observability of the unmanned helicopter are described. The closed-loop control law of attitude control loop and speed control loop is designed introducing state feedback, and the helicopter is transformed from static unstable object to stable controllable object. Secondly, the motion simulation strategy of unmanned helicopter based on 6-DOF motion simulation platform is illustrated. Finally, the validity of the method is verified by combining the mathematical model of the unmanned helicopter with the 6-DOF motion platform. Compared to traditional control algorithms, composite control design improves the anti-interference dynamic characteristics and steady-state performance of closed-loop systems by more than 50%. Adjusting time, mean squared error, increase percentage of the angular motion response curves is 2.34 s, 0.0012,

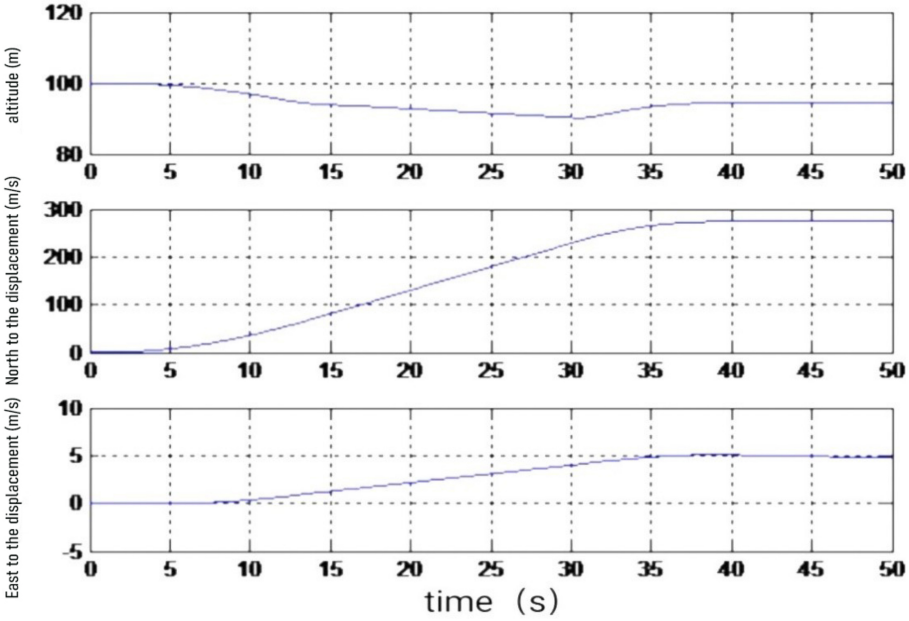


Figure 7. The displacement response curve of helicopter flight mode.

Table 2
Performance Parameter Comparison

| | Classification | Adjusting time | Mean squared error | Increase percentage |
|---|---|---|---|---|
| 1 | The angular motion response curves of helicopter take-off and hover modes | 2.34 | 0.0012 | 63.61% |
| 2 | The velocity response curves of helicopter take-off and hover modes | 2.47 | 0.0008 | 71.43% |
| 3 | The displacement response curves of helicopter take-off and hover modes | 2.32 | 0.0011 | 82.62% |
| 4 | The angular motion response curve of the helicopter direct flight mode platform | 7.42 | 0.0288 | 82.22% |
| 5 | The velocity response curve of the helicopter direct flight mode platform | 6.43 | 0.0042 | 84.97% |
| 6 | The displacement response curve of helicopter flight mode | 14.21 | 0.0045 | 75.82% |

63.61%, respectively. Adjusting time, mean squared error, increase percentage of the velocity response is 2.47 s, 0.0008, 71.43%, respectively. Adjusting time, mean squared error, increase percentage of the displacement response curves is 2.32 s, 0.0011, 82.62%, respectively. The closed-loop control system has asymptotic stability, and MATLAB simulation has verified that the algorithm proposed in the paper has good performance.

## Acknowledgment

This work was supported by Cooperative Project of Jiangsu Province production, teaching and research (No. BY2021381), Jinling Institute of Technology Ph. D. Startup Fund (jit-b-202314).

## References

[1] Y. Fang, Development prospects for unmanned helicopter systems, *Aeronautical Science and Technology, 32(*1), 2021, 35–40.

[2] M. Wan, M. Chen, and K. Yong, Adaptive tracking control for an unmanned autonomous helicopter using neural network and disturbance observer, *Neurocomputing, 468*(2), 2022, 296–305.

[3] A.F. A.J. Hasan, Humaidi, A.Sh. Mahdi Al-Obaidi, A.T. Azar, I.K. Ibraheem, A.Q. Al-Dujaili, A.K. Al. Mhdawi, and F.A. Abdulmajeed, Fractional order extended state observer enhances the performance of controlled tri-copter UAV based on active disturbance rejection control, in *Mobile robot: Motion control and path planning*, (Cham: Springer, 2023), 439–487.

[4] W. Zheng, Prediction and analysis of robotic arm trajectory based on adaptive control, *Mechatronic Systems and Control, 51*(10), 2023, 1–9.

[5] N. Gupta and L. Dewan, Trajectory tracking and balancing control of rotary inverted pendulum system using quasi-sliding

mode control, *Mechatronic Systems and Control, 50*(1), 2022, 1–8.

[6] R. Ding, C. Ding, Y. Xu, W. Liu, and X. Yang, Neural network-based robust integral error sign control for servo motor systems with enhanced disturbance rejection performance, *ISA Transactions, 129*, 2022, 580–591.

[7] B. Wang, C. Cao, Q. Zhao, X. Yuan, and Z. Zhu, Aeroacoustic characteristic analyses of coaxial rotors in hover and forward flight, *International Journal of Aeronautical and Space Sciences, 22*(6), 2021, 1278–1292.

[8] J. Seo, S. Lee, J. Lee, and J. Choi, Nonaffine helicopter control design and implementation based on a robust explicit nonlinear model predictive control, *IEEE Transactions on Control Systems Technology, 30*(2), 2022, 811–818.

[9] J. Hou, M. Chen, and N. Liu. Unmanned helicopter control based on radial basis function neural network and extended state observer, *Control Theory & Applications, 38*(9), 2021, 1361–1371.

[10] K.B. Kidambi, C. Fermüller, Y. Aloimonos, and H. Xu, Robust nonlinear control based trajectory tracking for quad rotors under uncertainty, *IEEE Control Systems Letters, 5*(6), 2021, 2042–2047.

[11] Y. Wei, H. Deng, and Z. Pan, Research on a combinatorial control method for coaxial rotor aircraft based on sliding mode, *Defence Technology, 18*(2), 2022, 280–292.

[12] S.I. Abdelmaksoud, M. Mailah, and M. Abdallaha. Control strategies and novel techniques for autonomous rotorcraft unmanned aerial vehicles: A review, *IEEE Access, 8*, 2020, 195142–195169.

[13] L. Yu, G. He, X. Wang, and S. Zhao, Robust fixed-time sliding mode attitude control of tilt tri-rotor UAV in Helicopter mode, *IEEE Transactions on Industrial Electronics, 69*(10), 2021, 10322–10332.

[14] W. Xu and F. Zhang, Fast-LIO: A fast, robust LiDAR-inertial odometry package by tightly-coupled iterated kalman filter, *IEEE Robotics and Automation Letters, 6*(2), 2021, 3317–3324.

[15] X. Zhu and D. Li, Robust fault estimation for a 3-DOF helicopter considering actuator saturation, *Mechanical Systems and Signal Processing*, *155*, 2021, 107624.

[16] Z. Wang, X. Zhou, C. Xu, and F. Gao, Geometrically constrained trajectory optimization for multi copters, *IEEE Transactions on Robotics, 38*(5), 2022, 3259–3278.

[17] A. Romero, R. Penicka, and D. Scaramuzza, Time-optimal online replanning for agile quadrotor flight, *IEEE Robotics and Automation Letters, 7*(3), 2022, 7730–7737.

[18] T. Krebs, G. Bramesfeld, and J. Cole, Transient thrust analysis of rigid rotors in forward flight, *Aerospace, 9*(1), 2022, 28.

[19] X.M. Zheng and C.Y. Ma, An intelligent target detection method of UAV swarms based on improved KM algorithm, *Chinese Journal of Aeronautics, 34*(2), 2021, 539–553.

[20] L.Q. Wang, H. Xu, Y.C. Zhang, and S. Shen, Neither fast nor slow: how to fly through narrow tunnels, *IEEE Robotics and Automation Letters, 7*(2), 2022, 5489–5496.

[21] A. Basiri, V. Mariani, G. Silano, M. Aatif, L. Iannelli, and L. Glielmo, A survey on the application of path-planning algorithms for multi-rotor UAVs in precision agriculture, *The Journal of Navigation, 75*(2), 2022, 364–383.

[22] W. Liang, Z. Chen, and B. Yao, Geometric adaptive robust hierarchical control for quadrotors with aerodynamic damping and complete inertia compensation, *IEEE Transactions on Industrial Electronics, 69*(12), 2022, 13213–13224.

## Biographies

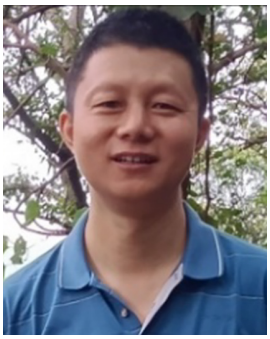

*Hongcheng Zhou* received the Ph.D. degree in control science in 2016. He is working as an Associate Professor with the School of Electronic and Information Engineering, Jinling Institute of Technology. He has published more than 10 articles in Chinese core journals and foreign engineering index source journals. His areas of interest include fault diagnosis, fault-tolerant control, data-driven control, and system identification.